



Power and motion control of a floating wind turbine: an original approach based on adaptive second order sliding mode control

Cheng Zhang, Franck Plestan

► To cite this version:

Cheng Zhang, Franck Plestan. Power and motion control of a floating wind turbine: an original approach based on adaptive second order sliding mode control. IFAC World Congress, 2020, Berlin, Germany. hal-02561414

HAL Id: hal-02561414

<https://hal.science/hal-02561414>

Submitted on 24 Apr 2023

HAL is a multi-disciplinary open access archive for the deposit and dissemination of scientific research documents, whether they are published or not. The documents may come from teaching and research institutions in France or abroad, or from public or private research centers.

L'archive ouverte pluridisciplinaire **HAL**, est destinée au dépôt et à la diffusion de documents scientifiques de niveau recherche, publiés ou non, émanant des établissements d'enseignement et de recherche français ou étrangers, des laboratoires publics ou privés.



Distributed under a Creative Commons Attribution - NonCommercial 4.0 International License

Power and motion control of a floating wind turbine: an original solution based on adaptive second order sliding mode control

C. Zhang* F. Plestan*

** École Centrale de Nantes - LS2N, UMR CNRS 6004, Nantes, France.
E-mail: {Cheng.Zhang, Franck.Plestan}@ec-nantes.fr.*

Abstract: A new control scheme based on adaptive super-twisting algorithm is proposed for a floating wind turbine equipped by a permanent magnet synchronous generator. The adaptive control method is especially efficient for systems with uncertainties and external perturbations and, therefore, is well adapted to wind turbines systems. Such controller can be implemented with very limited knowledge of system model (only the relative degree is required) that greatly reduces the controller gains tuning effort. Simulations are made on FAST software and compared with a standard gain-scheduled PI controller.

Keywords: Super-twisting algorithm, adaptive gain, floating wind turbine.

1. INTRODUCTION

Over the last decade, floating wind turbines (FWTs) emerge as a focus of research of renewable energy. The control system plays an important role in such large wind turbine systems. However, the standard control strategies developed for onshore wind turbines (as collective blade pitch (CBP) control) in above rated region can not be directly used on FWT due to the negative damping on the platform motion (Nielsen et al. 2006). Therefore, new control scheme must be developed given that the control objectives of FWTs in the above rated region are not only to ensure the rated power production, but also to reduce the platform motion. Notice that a key-point in such systems is the limitation of the structure fatigue load.

Many works have been made in the FWTs field, in (Jonkman 2008), the platform pitch motion is reduced thanks to a gain scheduling PI (GSPI) controller. In Lackner (2009), the control scheme is made such that the rotor speed is set as a function of the platform pitch velocity whereas the generator torque is forced to its rated value; by this way, the platform pitching is reduced but the cost is larger power fluctuations. Linear control algorithms have been mainly used in the control of FWTs, such as linear quadratic regulator (Namik et al. 2008), model predictive control and feed-forward control (Schlipf et al. 2012, 2015). Some works have used additional control inputs such as individual blade pitch (IBP) angle or generator torque (Namik and Stol 2014, Suemoto et al. 2017). However, most part of the controllers are based on linear models of FWTs around an operating point (depending on wind condition and rotor speed), the efficiency of the controller being guaranteed in a limited operating domain. Consequently, in order to keep an interest over a larger operating domain, controller gains must be changed versus operating conditions, to keep the efficiency (see for example GSPI). The task of controllers tuning appears to be fastidious. A solution to avoid this task is the use of nonlinear controllers, potentially based on nonlinear models. Thus, in (Sandner et al. 2012, Homer and Nagamune 2017),

nonlinear models have been developed, but their use is limited in the frame of control.

Another approach consists in using robust controllers that can be applied to (linear or nonlinear) systems for which the knowledge is very limited. Concerning robust control, a class of such controllers is the sliding model control (SMC) one (Utkin 1977, Utkin et al. 2009). Among the numerous SMC algorithms (first order, second order, high order), the control law selected in this paper is the adaptive version (Shtessel et al. 2012) of the popular super-twisting (STW) (Levant 1993). This second order sliding mode controller has several features that are well-adapted to FWTs control problem: it ensures the establishment of a second order sliding mode, that improves the accuracy with respect to standard sliding mode control; it offers a continuous control that reduces the chattering phenomenon, thereby well protected the actuators; it is an output feedback controller that reduces the use of time derivative of the sliding variable with respect to other second order sliding mode control laws; the controller gains can be dynamically adapted with respect to perturbations and uncertainties; and finally, the adaptive gains allow to have a very reduced knowledge of the system that can be nonlinear.

This kind of control strategies have been very recently and successfully applied by the authors to a FWT, but without considering the electrical part of the wind turbine. In these previous works (Zhang et al. 2019a,b), several gain adaptation strategies for super-twisting controller have been used for the control of FWT, by considering only the aero/hydrodynamic part (electrical part of the FWT is not taken into account - it is supposed that the torque applied to turbine is constant). The control design has been made by supposing that only the relative degree of the control objective is known (that is a very limited information). This approach is totally new in the context of FWTs. Indeed, both these papers have shown that the use of such controllers allows to reach higher performances versus GSPI, even if the knowledge of the system is very reduced.

In the current paper, a permanent magnet synchronous generator is now included in the system. A control based on adaptive super twisting algorithm is applied for the very first time to complete model of FWT including aerodynamic, hydrody-

* The work of Cheng Zhang is financially supported by CSC (Chinese Scholarship Council).

namic and electrical parts and, such control scheme combined the collective blade pitch angle control and the generator torque control.

2. MODELLING OF THE SYSTEM

The wind turbine considered in this work is the National Renewable Energy Laboratory (NREL) 5MW OC3-Hywind, supported by a spar-buoy platform that is modeled by an open-source software FAST (Fatigue, Aerodynamics, Structures and Turbulence) (see details in (Jonkman et al. 2009, Jonkman 2010)). The model used in FAST is highly nonlinear, complex and not adapted for the control design; a reduced model can be used as detailed in the sequel. Furthermore, permanent magnet synchronous generator (PMSG) is supposed to be installed in the FWT.

2.1 Models of floating wind turbine

The mechanical dynamics of the wind turbine reads as

$$\begin{aligned}\dot{\Omega}_r &= \frac{1}{J}(T_a - \eta T_g) \\ \Omega_g &= \eta \Omega_r\end{aligned}\quad (1)$$

with Ω_r , T_a , Ω_g and T_g the rotor speed, the aerodynamic torque of rotor, the generator speed and the generator torque respectively, J the overall inertial and η the ratio of gear box that connects both the shafts of turbine rotor and generator. Aerodynamic torque T_a can be written as a function of power coefficient $C_p(\lambda, \beta)$ (Huang et al. 2015, Guenoune et al. 2017)

$$T_a = \frac{1}{2} \frac{C_p(\lambda, \beta)}{\lambda} \rho \pi R^3 V^2 \quad (2)$$

with ρ ($1.255 \text{ kg} \cdot \text{m}^{-3}$) the air density, R the radius of wind turbine blade, V the wind speed, β the blade pitch angle. λ is the tip-speed ratio reading as

$$\lambda = \frac{\Omega_r R}{V} \quad (3)$$

The power coefficient $C_p(\lambda, \beta)$ can be described by

$$\begin{aligned}C_p &= c_1(c_2\xi - c_3\beta - c_4)e^{c_5\xi} \\ \xi &= \frac{1}{\lambda + 0.08\beta} - \frac{0.035}{\beta^3 + 1}\end{aligned}\quad (4)$$

with $c_1 - c_5$ the C_p curve fitting coefficients (for details, see Guenoune et al. (2017)). These latter coefficients depend on the wind turbine and are estimated among large scale of simulations. As conclusion, it is clear that C_p is not well-known and introduces uncertainties in the model.

Notice that, according to (1)-(4), rotor speed Ω_r can be controlled by actuating on the blade pitch angle β , and thereby regulate the power output in the considered region. Indeed, the blade pitch angle β explicitly appears in the first time derivative of Ω_r through T_a ; it means that the relative degree (Isidori 2013) of Ω_r with respect to β equals to 1. However, the formal relation is very difficult to be precisely established.

Furthermore, in the previous modelling, the hydrodynamics, *i.e.* the floating part of the system, is not taken into account. Notice that hydrodynamic models of the floating platform proposed in the literature, such as (Betti et al. 2013, Sandner et al. 2012), are limited in the frame of control.

A linear model (5) can be derived by FAST software. Such model is got thanks to linearization around an operating point

(depending on wind and rotor speed conditions). Considering a limited degree of freedom and the variations around the operating point composed by platform pitch angle ϕ_o and its velocity $\dot{\phi}_o$, rotor speed Ω_{ro} and blade pitch angle u_o , one gets the following linear dynamics

$$\dot{\Delta x} = A \cdot \Delta x + B \cdot \Delta \beta + \Delta \delta \quad (5)$$

with Δx the system state vector, composed by the variations around the operating point of the platform pitch $\Delta \phi$, platform pitch rate $\Delta \dot{\phi}$ and rotor speed $\Delta \Omega_r$, $\Delta \beta$ being the variation of collective blade pitch angle. Given the term $\Delta \delta$ that describes the perturbations on the FWT, the model (5) is viewed as a perturbed linear one. The system matrices A and B are obtained from the FAST software, their values depending on the considered operating point. As example, for a wind speed equal to 16 m/s and a rotor speed equal to its rated value Ω_{ro} , one has

$$A = \begin{bmatrix} 0 & 1 & 0 \\ -0.0141 & -0.0402 & -0.0003 \\ -0.0525 & -2.0615 & -0.1624 \end{bmatrix}, B = \begin{bmatrix} 0 \\ -0.0033 \\ -0.9479 \end{bmatrix} \quad (6)$$

whereas, for a wind speed equal to 18 m/s with the same rotor speed, one gets

$$A = \begin{bmatrix} 0 & 1 & 0 \\ -0.0141 & -0.0405 & -0.0004 \\ -0.0757 & -2.3031 & -0.2304 \end{bmatrix}, B = \begin{bmatrix} 0 \\ -0.0035 \\ -1.1864 \end{bmatrix} \quad (7)$$

Notice that, from (6) or (7), it is confirmed that the relative degree of the rotor velocity versus the blade pitch angle equals to 1. Consequently, due to the wind variations and considering a large operating domain, it is reasonable to assume the FWT model as follows

$$\dot{x} = A(t) \cdot x + B(t) \cdot \beta + \delta \quad (8)$$

with $x = [\phi \ \dot{\phi} \ \Omega_r]^T$ and δ the perturbation term including all the uncertainties, and external perturbations (waves and wind effect, ...). By a more general point-of-view, the previous system can be viewed as a class of nonlinear system reading as

$$\dot{x}_{wt} = f_{wt}(x_{wt}, t) + g_{wt}(x_{wt}, t)u_{wt} + \delta \quad (9)$$

with $x_{wt} = [\phi \ \dot{\phi} \ \Omega_r]^T$, $u_{wt} = \beta$, $f_{wt}(x_{wt})$ including the term with δ and $g_{wt}(x_{wt})$ being uncertain and unknown. One can also assume that

- from (5)-(7), both the rotor speed Ω_r and platform pitch velocity $\dot{\phi}$ can be controlled by blade pitch angle β . Furthermore, the relative degree of Ω_r and $\dot{\phi}$ equals to 1;
- $f_{wt}(x_{wt}, t)$ and $g_{wt}(x_{wt}, t)$ are bounded because the wind speed and rotor speed are limited.

2.2 Model of the electrical machine

The permanent magnet synchronous generator model in the $d-q$ frame reads as (Guenoune et al. 2017)

$$\begin{aligned}\dot{i}_d &= -\frac{R_s}{L_d}i_d + \frac{pL_q}{L_d}\Omega_g i_q + \frac{1}{L_d}V_d \\ \dot{i}_q &= -\frac{R_s}{L_q}i_q - \frac{pL_d}{L_q}\Omega_g i_d - \frac{p\phi_f}{L_q}\Omega_g + \frac{1}{L_q}V_q\end{aligned}\quad (10)$$

with i_d , i_q , V_d , V_q the currents and the voltages along the $d-q$ axes respectively, L_d and L_q the inductance. R_s , p and ϕ_f are respectively the stator resistance, the number of pole pairs and the permanent-magnet flux linkage. Then, as the wind turbine, the electrical machine reads as a nonlinear system such that

$$\dot{x}_{em} = f_{em}(x_{em}, t) + g_{em}(x_{em}, t)u_{em} \quad (11)$$

with $x_{em} = [i_d \ i_q]^T$, $u_{em} = [V_d \ V_q]^T$, $f_{em}(x_{em}, t)$ and $g_{em}(x_{em}, t)$ being uncertain and not well-known.

3. PROBLEM STATEMENT

In the above rated region (often named Region III), the first control objective is the regulation of the power at its rated value: in other words, the objective is to limit the power in order to protect the electric machine and the mechanical structure. On the other hand, the floating platform pitch motion can induce instability and increases load fatigue. As a consequence, it is necessary to reduce the platform pitch motion, *i.e.* to reduce platform pitch velocity.

3.1 Rotor speed reference

From (5)-(7), the two control objectives, *i.e.* rotor speed and platform pitch velocity, have to be achieved by a single control input (collective blade pitch angle). A solution to solve such problem is to take advantage of the physical features of the floating wind turbine. Consider that the desired rotor speed Ω_r^* is a function of platform pitch velocity as

$$\Omega_r^* = \Omega_{ro} - k \cdot \dot{\phi} \quad (12)$$

where Ω_{ro} is the rated rotor speed ($\Omega_{ro} = 12.1$ rpm) and k is a positive constant. The idea of such reference makes use of the trade-off between rotor speed and platform pitch. Suppose that $\Omega_r^* = \Omega_{ro}$ and the control is efficient, *i.e.* $\Omega_r = \Omega_r^*$. Now, $\dot{\phi}$ becomes negative: therefore, from (12), Ω_r^* increases. Therefore, the aerodynamic force that is opposite to the tower motion, increases. Then, $|\dot{\phi}|$ is reduced: from (12), Ω_r^* decreases. The system naturally reduces the pitch motion (Lackner 2009, Cunha et al. 2014), and so on.

3.2 Direct current reference

The existence of large direct current i_d induces oscillations of the electromagnetic torque: such oscillations can degrade the power production and increase the fatigue loads of the shafts (Bose 1988). Therefore, the current i_d must be forced to zero in order to avoid those negative effects.

3.3 Quadratic current reference

Denoting P_o the rated power, the corresponding generator torque reads as

$$T_g^* = \frac{P_o}{\eta \Omega_r} \quad (13)$$

Meanwhile, the generator torque is defined as

$$T_g = \frac{3}{2} p \phi_f i_q \quad (14)$$

Hence, one can conclude that the control of generator torque is equivalent to the control of i_q . Therefore, from (13)-(14), if the objective is to limit the power to its rated value, the reference of i_q reads as

$$i_q^* = \frac{2P_o}{3\eta\Omega_r p\phi_f} \quad (15)$$

4. CONTROL DESIGN

The floating wind turbine system withstands not only the system uncertainties due to flexible structures, but also the influence of wind and waves. Hence, such system is highly perturbed, uncertain and nonlinear. The linear controller proposed in the literature, such as GSPI, is designed based on the linearized model around an operating point: it is efficient while

system is evolving around the range of this point. However, a large set of gains must be tuned in order to keep the control efficiency at different operating points that increases the tuning effort. It is necessary to design a nonlinear robust controller with a *single* set of parameters tuning meanwhile keeping the control efficiency among the large operating range despite of the uncertainties and perturbations. Furthermore, the controller design must require a very limited knowledge on the system.

Hence, the previous mentioned super-twisting algorithm is adopted, in addition, given the unknown terms of the rotor and platform pitch dynamics, the uncertainties on turbine and electrical machine, the external perturbations, the controllers gains must be chosen sufficiently large to accommodate those effects. This fact gives a “high gain” control that induce chattering and degrade the controller performance. Therefore, adaptive version of STW Shtessel et al. (2012) is used: it allows to dynamically adapt the gain versus uncertainties and perturbations while keeping high level of performances, even in case of very reduced knowledge of the system.

4.1 Recalls

Consider the following system

$$\begin{aligned} \dot{z} &= f(z) + g(z)v \\ y &= S(z, t) \end{aligned} \quad (16)$$

with $z \in Z \subset \mathbb{R}^n$ the state and $v \in U \subset \mathbb{R}$ the control input, f and g the bounded unknown nonlinear functions, y the system output. Define $S(z, t)$, called the “sliding variable” and defined such that, once $S = 0$, then $y \rightarrow 0$.

The idea of SMC is to design the control input v such that the sliding variable $S(z, t)$ is forced to reach the sliding surface $S(z, t) = 0$ in a finite time, in spite of uncertainties and perturbations. Once $S(z, t) = 0$, the system trajectories are evolving on this surface, and y goes towards 0. Notice that the sliding variable $S(z, t)$ is defined according to control objective y and its relative degree. Assume that

Hypothesis 1. The relative degree of system (16) equals to 1. ■

Define $S = y$: one gets

$$\dot{S} = \underbrace{\frac{\partial S}{\partial t} + \frac{\partial S}{\partial z} f(z)}_{a(z, t)} + \underbrace{\frac{\partial S}{\partial z} g(z)}_{b(z, t)} v \quad (17)$$

Hypothesis 2. $a(z, t)$ and $b(z, t)$ are unknown but bounded functions, such that $|a| \leq a_M$, $0 \leq b_m \leq b \leq b_M$ for $z \in Z$ and $t > 0$, a_M , b_m and b_M being the positive constant. ■

The objective now is to drive sliding variable S to zero thanks to the control v . The Super-twisting algorithm (Levant 1993) given by

$$\begin{aligned} v &= -k_1 |S|^{\frac{1}{2}} \cdot \text{sign}(S) + w \\ \dot{w} &= -k_2 \cdot \text{sign}(S) \end{aligned} \quad (18)$$

with k_1 and k_2 the controller gains

$$k_1 > \frac{a_M}{b_M}, \quad k_2 \geq \frac{4a_M}{b_m^2} \cdot \frac{b_M}{b_m} \cdot \frac{k_1 + a_M}{k_1 - a_M} \quad (19)$$

ensures $S = \dot{S} = 0$ in a finite time¹. It is clear that the sliding mode can be established in a finite time with sufficiently large

¹ In practice, the supertwisting controller ensures, in a finite time, the establishment of a “real” second order sliding mode (Levant 1993), *i.e.* $|S| < \mu_1 T_e^2$, $|\dot{S}| < \mu_2 T_e$ with T_e the control sampling time, μ_1 and μ_2 positive constant.

gains. However, in practice, the bounds of uncertainties and perturbations are difficult to determine; furthermore, even if they are determined, they are often over-estimated that degrade the control performance.

A solution is to use adaptive gains strategy: it allows to increase the gains when accuracy is not sufficient, and to reduce them when control objectives are reached. An adaptive version of the super-twisting (ASTW) controller has been proposed in Shtessel et al. (2012) and reads as (18) with the gains k_1 and k_2 defined as

$$\begin{aligned} \dot{k}_1 &= \begin{cases} \omega \sqrt{\frac{\chi}{2}} \text{sign}(|S| - \mu) & \text{if } k_1 > k_{1m} \\ k & \text{if } k_1 < k_{1m} \end{cases} \\ k_2 &= \varepsilon k_1 \end{aligned} \quad (20)$$

with k_{1m} , ε , ω , χ , μ and k positive constants. Furthermore, $k_1(0) > k_{1m}$. The idea of the adaptation law (20) is the following

- if $|S| > \mu$, it means that the accuracy is low. Then, it could be due to a low gain: k_1 (and then k_2) is increased;
- if $|S| < \mu$, it means that the accuracy is good. Then, it means that the gain is enough large and could be reduced: k_1 (and then k_2) is decreased;
- if k_1 becomes very small, and in order to guarantee its positiveness, k_1 is smoothly increased.

4.2 Application to floating wind turbine

As described in Section 2 by (9)-(11), the control input vector u and the output vector y of the whole system read as

$$u = \begin{bmatrix} \beta \\ V_d \\ V_q \end{bmatrix}, \quad y = \begin{bmatrix} y_1 \\ y_2 \\ y_3 \end{bmatrix} = \begin{bmatrix} \Omega_r - \Omega_r^* \\ i_d - i_d^* \\ i_q - i_q^* \end{bmatrix} \quad (21)$$

Recalling that the control objective is to ensure $y \rightarrow 0$ and the relative degree of the outputs y_1 , y_2 and y_3 with respect to u equal to 1, the sliding variable vector S is defined as

$$S = [S_1 \ S_2 \ S_3]^T = [y_1 \ y_2 \ y_3]^T \quad (22)$$

Therefore, time derivatives of S read as

$$\begin{aligned} \dot{S}_1 &= \frac{1}{2J} \left(\frac{C_p(\lambda, \beta)}{\Omega_r} \rho \pi R^2 V^3 - 3\eta p \phi_f i_q \right) + k\ddot{\phi} \\ \dot{S}_2 &= -\frac{R_s}{L_d} i_d + \frac{pL_q}{L_d} \Omega_g i_q + \frac{1}{L_d} V_d \\ \dot{S}_3 &= -\frac{R_s}{L_q} i_q - \frac{pL_d}{L_q} \eta \Omega_g i_d - \frac{p\phi_f}{L_q} \eta \Omega_g - \frac{2P_o \dot{\Omega}_r}{3\eta p \phi_f \Omega_r^2} + \frac{1}{L_q} V_q \end{aligned} \quad (23)$$

Dynamics of S_1 depends on C_p and $\ddot{\phi}$ is not well-known. Furthermore, it can be numerically shown that, in the operating domain and from (4), the power C_p can be approximated as

$$C_p = C_{p1}(\cdot) + C_{p2}(\cdot)\beta \quad (24)$$

Consequently, the dynamic of S_1 can be rewritten as

$$\dot{S}_1 = a_1(\cdot) + b_1(\cdot)\beta \quad (25)$$

with a_1 and b_1 unknown but bounded functions.

Dynamics of S_2 can be rewritten from the second equation of (23) as

$$\dot{S}_2 = a_2(\cdot) + b_2(\cdot)V_d \quad (26)$$

Note that, in the model (10) of PMSG, each parameter is composed by a known nominal part and unknown uncertainty one (for example, the resistance R_s can be written as $R_s =$

$R_{sn} + \Delta R_s$, R_{sn} being its nominal value and ΔR_s the associated uncertainty). Then, one gets

$$a_2 = a_{2n} + \Delta a_2, \quad b_2 = b_{2n} + \Delta b_2 \quad (27)$$

with a_{2n} and b_{2n} the nominal part and a_{2u} and b_{2u} the uncertainty part. The terms a_{2n} and b_{2n} read as²

$$a_{2n} = -\frac{R_s}{L_d} i_d + \frac{pL_q}{L_d} \Omega_g i_q, \quad b_{2n} = \frac{1}{L_d} \quad (28)$$

Dynamics of S_3 depends on the dynamics of Ω_r that is not well-known and coupled with the blade pitch angle β . However, numerical analysis in the operating domain shows that the influence of β is very limited on S_3 dynamics. Therefore, consider the term in \dot{S}_3 that contains $\dot{\Omega}_r$ as a bounded perturbation which gives

$$\dot{S}_3 = a_3(\cdot) + b_3(\cdot)V_q \quad (29)$$

with $a_3 = a_{3n} + \Delta a_3$ and $b_3 = b_{3n} + \Delta b_3$. The terms a_{3n} and b_{3n} read as

$$a_{3n} = -\frac{R_s}{L_q} i_q - \frac{pL_d}{L_q} \eta \Omega_g i_d - \frac{p\phi_f}{L_q} \eta \Omega_g, \quad b_{3n} = \frac{1}{L_q} \quad (30)$$

Therefore, the control input reads as

$$u = \begin{bmatrix} \beta \\ V_d \\ V_q \end{bmatrix} = \begin{bmatrix} v_1 \\ \frac{1}{b_{2n}}(-a_{2n} + v_2) \\ \frac{1}{b_{3n}}(-a_{3n} + v_3) \end{bmatrix} \quad (31)$$

with v_1 , v_2 and v_3 based on the ASTW algorithm (18)-(20)

$$\begin{bmatrix} v_1 \\ v_2 \\ v_3 \end{bmatrix} = \begin{bmatrix} -k_{11}|S_1|^{\frac{1}{2}} \text{sign}(S_1) - \int_0^t k_{12} \text{sign}(S_1) d\tau \\ -k_{21}|S_2|^{\frac{1}{2}} \text{sign}(S_2) - \int_0^t k_{22} \text{sign}(S_2) d\tau \\ -k_{31}|S_3|^{\frac{1}{2}} \text{sign}(S_3) - \int_0^t k_{32} \text{sign}(S_3) d\tau \end{bmatrix} \quad (32)$$

with the gains k_{11}, k_{21}, k_{31} and k_{12}, k_{22}, k_{32} respectively defined as k_1 and k_2 in (20).

4.3 GSPI+PI control

The control of rotor speed considered in this paper is the baseline GSPI controller, it is regarded as a comparison object. The control objective being to regulate rotor speed at its rated value Ω_{ro} that gives

$$v_1 = \eta k_p (\Omega_r - \Omega_{ro}) + \eta k_i \int_0^t (\Omega_r - \Omega_{ro}) d\tau \quad (33)$$

with k_p and k_i obtained for different operating points and scheduled as functions of blade pitch angle; the gains and the gain scheduled PI are derived from (Jonkman 2008) in order to avoid platform pitch resonance.

The control of direct current/power control is as stated in Section 3.3 with a PI controller, then, the control inputs v_2 and v_3 are defined as

$$\begin{aligned} v_2 &= k_{p2} S_2 + k_{i2} \int_0^t S_2(\tau) d\tau \\ v_3 &= k_{p3} S_3 + k_{i3} \int_0^t S_3(\tau) d\tau \end{aligned} \quad (34)$$

² These expressions are given with the nominal values of all the parameters.

5. SIMULATIONS AND RESULTS

5.1 Benchmark

Simulations are made thanks to the co-simulation between MATLAB/SIMULINK and FAST nonlinear model. All DOFs of the FAST nonlinear model are enabled. The parameters of the FWT can be found in (Jonkman et al. 2009); the PMSG has 5 pairs of pole with stator resistance, stator inductance and flux linkage equal to 1.06Ω , 14.29 mH and 8.6 Wb respectively. Two kind of controllers are compared

- **GSPI+PI**: rotor speed GSPI (33) with power/direct current control (34);
- **ASTW**: super-twisting algorithm (31)-(32) with gain adaptation proposed in Sections 4.1 and 4.2.

All the simulations are under same conditions: 18 m/s stochastic wind with 15% turbulence intensity; irregular wave with significant height of 3.25 m , peak spectral period of 9.7 s ; since there is no blade dynamic in the FAST model, the blade pitch angle is saturated between $[0^\circ, 90^\circ]$, and the associated rate is limited between $[-8^\circ, 8^\circ]$.

5.2 Results and Discussion

All the performances indicators of are normalized and are shown in Figure 1. Figure 1-top including the root mean square (RMS) of power error, platform pitch rate and platform motions; the variation (VAR) of blade pitch angle that indicates the use of blade pitch actuator. Figure 1-bottom displays the standard deviation (STD) of tower base (TB) moments in fore-aft, side-to-side and torsional directions, the STD of blade root (BR) edge-wise and flap-wise moments. For all the indicators, the smaller the values are, the better the performances are.

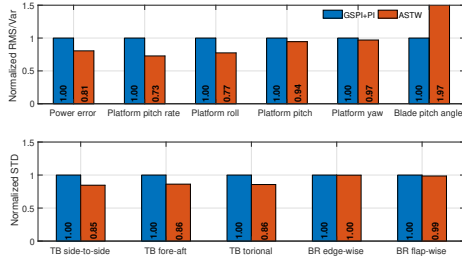


Fig. 1. Normalized performances indicators with GSPI+PI (blue) and ASTW (red) controllers.

It is clear that the ASTW proposed in this work greatly reduced the power fluctuation and the platform pitch motion comparing with GSPI+PI controller, by 19% and 27% respectively (see Figure 1-top); furthermore, the tower base side-to-side, fore-aft and torsional fatigue load are 15%, 14% and 13% less than GSPI+PI (see Figure 1-bottom). Both controllers have similar influence on blade flap-wise deflection and the blade root load. Overall, according to the simulation results, the ASTW performs better than GSPI+PI controller. The most significant cost of such improvement is the more usage of the blade pitch actuator, *i.e.* the blade pitch angle variation is increased by 97% (see Figure 1-top). Nonetheless, such increase is acceptable for the blade pitch actuator, since the control is applied under the saturation of blade pitch angle and its rate; furthermore,

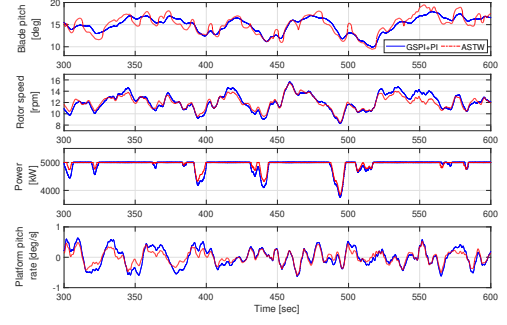


Fig. 2. FWT variables versus time (sec.) obtained by GSPI+PI (blue) and ASTW (red) controllers.

recall that the tuning of the sliding mode control is simpler (a single tuning for the whole operating domain). One can find the trajectories of main system variables in Figure 2.

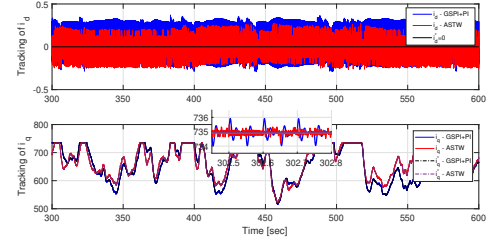


Fig. 3. Currents i_d (A) and i_q (A) obtained by GSPI+PI and ASTW controllers versus time (sec.).

The results of the electrical part are shown in Figure 3 and Table 1. ASTW allows smaller tracking errors on both i_d and i_q . In other words, the ASTW can keep better control efficiency in spite of perturbations than PI (see Figure 3). Figure 5 displays the stator voltages and currents. Indeed, PI control might improve the performance by using the gain-schedule technology as the turbine part control used, but a large scale of tuning must be done. Note that the ASTW control used in this work can keep good performance with a single phase of tuning thanks to its adaptation. Indeed, the controller gains are dynamically adapted versus model uncertainties and perturbations (see Figure 4).

Table 1. Mean tracking error of PMSG currents.

Controller	Mean tracking error (A) of i_d	Mean tracking error (A) of i_q
GSPI+PI	0.0812	0.2157
ASTW	0.0536	0.1233

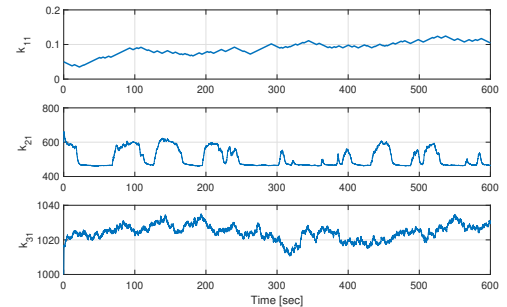


Fig. 4. Adaptive gains k_{11} , k_{21} and k_{31} versus time (sec.).

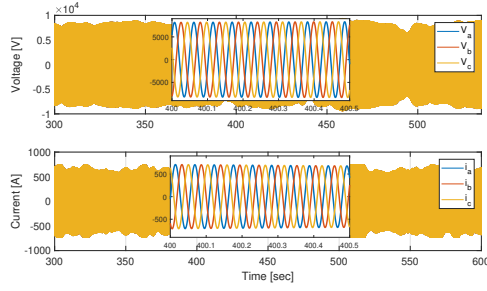


Fig. 5. Stator voltages (V) and currents (A) along the three phases frame versus time (sec.), by using ASTW controller.

6. CONCLUSION

Adaptive super-twisting algorithm is applied on the floating wind turbine equipped by a permanent magnet synchronous machine in above rated region. The proposed controller is evaluated on FAST software and has better performances on the power regulation, platform pitch motion and direct current reduction than baseline GSPI controller. The main features of ASTW controller are that very few information of the system model is required, and the controller tuning is simplified given that controller gains are dynamically adapted with respect to uncertainties and perturbations.

REFERENCES

- Betti, G., Farina, M., Guagliardi, G.A., Marzorati, A., and Scattolini, R. (2013). Development of a control-oriented model of floating wind turbines. *IEEE Transactions on Control Systems Technology*, 22(1), 69–82.
- Bose, B.K. (1988). A high-performance inverter-fed drive system of an interior permanent magnet synchronous machine. *IEEE Transactions on Industry Applications*, 24(6), 987–997.
- Cunha, A., Caetano, E., Ribeiro, P., and Müller, G. (2014). Reducing blade fatigue and damping platform motions of floating wind turbines using model predictive control. In *International Conference on Structural Dynamics*. Porto, Portugal.
- Guenoune, I., Plestan, F., Chermitti, A., and Evangelista, C. (2017). Modeling and robust control of a twin wind turbines structure. *Control Engineering Practice*, 69, 23–35.
- Homer, J.R. and Nagamune, R. (2017). Physics-based 3-d control-oriented modeling of floating wind turbines. *IEEE Transactions on Control Systems Technology*, 26(1), 14–26.
- Huang, C., Li, F., and Jin, Z. (2015). Maximum power point tracking strategy for large-scale wind generation systems considering wind turbine dynamics. *IEEE Transactions on Industrial Electronics*, 62(4), 2530–2539.
- Isidori, A. (2013). *Nonlinear control systems*. Springer Science & Business Media.
- Jonkman, J. (2008). Influence of control on the pitch damping of a floating wind turbine. In *AIAA Aerospace Sciences Meeting and Exhibit*. Reno, USA.
- Jonkman, J. (2010). Definition of the floating system for phase iv of oc3. Technical report, National Renewable Energy Lab.(NREL), Golden, CO (United States).
- Jonkman, J., Butterfield, S., Musial, W., and Scott, G. (2009). Definition of a 5-mw reference wind turbine for offshore system development. Technical report, National Renewable Energy Lab.(NREL), Golden, CO (United States).
- Lackner, M.A. (2009). Controlling platform motions and reducing blade loads for floating wind turbines. *Wind Engineering*, 33(6), 541–553.
- Levant, A. (1993). Sliding order and sliding accuracy in sliding mode control. *International journal of control*, 58(6), 1247–1263.
- Namik, H. and Stol, K. (2014). Individual blade pitch control of a spar-buoy floating wind turbine. *IEEE Transactions on Control Systems Technology*, 22(1), 214–223.
- Namik, H., Stol, K., and Jonkman, J. (2008). State-space control of tower motion for deepwater floating offshore wind turbines. In *46th AIAA Aerospace Sciences Meeting and Exhibit*, 1307.
- Nielsen, F.G., Hanson, T.D., and Skaare, B. (2006). Integrated dynamic analysis of floating offshore wind turbines. In *International Conference on Offshore Mechanics and Arctic Engineering*. Hamburg, Germany.
- Sandler, F., Schlipf, D., Matha, D., Seifried, R., and Cheng, P.W. (2012). Reduced nonlinear model of a spar-mounted floating wind turbine.
- Schlipf, D., Pao, L.Y., and Cheng, P.W. (2012). Comparison of feedforward and model predictive control of wind turbines using lidar. In *Conference on Decision and Control*. Hawaii, USA.
- Schlipf, D., Simley, E., Lemmer, F., Pao, L., and Cheng, P.W. (2015). Collective pitch feedforward control of floating wind turbines using lidar. *Journal of Ocean and Wind Energy*, 2(4), 223–230. doi:10.17736/jowe.2015.arr04.
- Shtessel, Y., Taleb, M., and Plestan, F. (2012). A novel adaptive-gain supertwisting sliding mode controller: Methodology and application. *Automatica*, 48(5), 759–769.
- Suemoto, H., Hara, N., and Konishi, K. (2017). Model-based design of individual blade pitch and generator torque controllers for floating offshore wind turbines. In *2017 11th Asian Control Conference (ASCC)*, 2790–2795. IEEE.
- Utkin, V. (1977). Variable structure systems with sliding modes. *IEEE Transactions on Automatic control*, 22(2), 212–222.
- Utkin, V., Guldner, J., and Shi, J. (2009). *Sliding mode control in electro-mechanical systems*. CRC press, Boca Raton, Florida, USA.
- Zhang, C., Gutierrez, S., Plestan, F., and de León-Morales, J. (2019a). Adaptive super-twisting control of floating wind turbines with collective blade pitch control. *IFAC-PapersOnLine*, 52(4), 117–122.
- Zhang, C., Tahoumi, E., Gutierrez, S., Plestan, F., and de León-Morales, J. (2019b). Adaptive robust control of floating offshore wind turbine based on sliding mode. In *Conference on Decision and Control*. Nice, France.

Appendix A. CONTROLLERS PARAMETERS

GSPI+PI. k_p and k_i are the same as Jonkman (2008) used. The gains of electrical part are $k_{p2} = 500$, $k_{i2} = 1e5$; $k_{p3} = 200$, $k_{i3} = 1e5$.

ASTW.

Gains	Parameters
k_{11}, k_{12}	$k_{1m} = 10^{-4}$, $\varepsilon = 0.03$, $\omega = 1$, $\chi = 0.001$, $\mu = 0.05$, $k = 10^{-4}$
k_{21}, k_{22}	$k_{1m} = 1$, $\varepsilon = 200$, $\omega = 1$, $\chi = 200$, $\mu = 0.05$, $k = 10$
k_{31}, k_{32}	$k_{1m} = 1$, $\varepsilon = 300$, $\omega = 1$, $\chi = 40$, $\mu = 0.1$, $k = 10$